Supporting information

Solvent influence structural variation from 3D 4-fold interpenetrated framework to 2D layer-type porous coordination polymer: Structure analysis and highly selective gas adsorption properties

Bo Liu, Hui Miao, Ling-Yan Pang, Lei Hou, Yao-Yu Wang,* and Qi-Zhen Shi

Key Laboratory of Synthetic and Natural Functional Molecule Chemistry of the Ministry of Education, Shaanxi Key Laboratory of Physico-Inorganic Chemistry, College of Chemistry & Materials Science, Northwest University. Xi'an 710069 (P. R. China).

Email: wyaoyu@nwu.edu.cn, Tel: 86 29 88302604

Table of Content

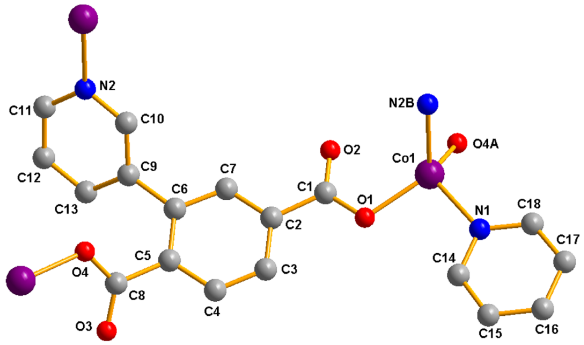

Fig. S1 The ball-and-stick drawing of the asymmetric unit in **1**, the hydrogen atoms and solvent molecules are omitted. Symmetry codes: A: x, -y, -1/2+z; B: -x, -y, 1-z.

a)

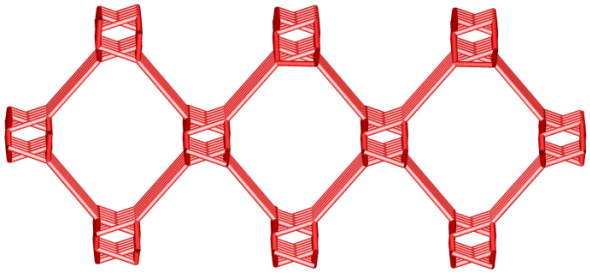

b)

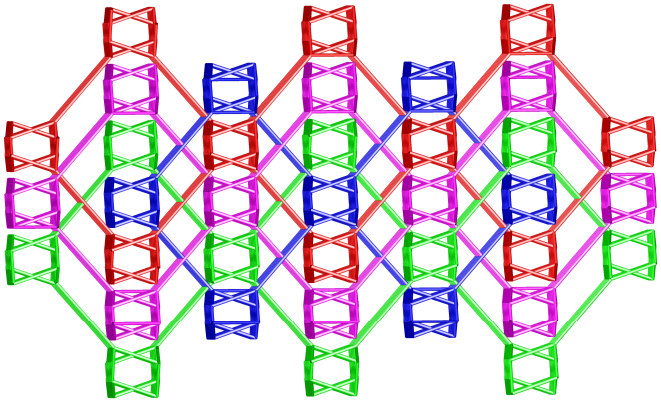

Fig. S2 Schematic representation of the single 3D net a), and the 4-fold interpenetrated net b) of **1** (each Co^{2+} acts as a four-connecting node and each $dcpy^{2-}$ as a three-connecting node).

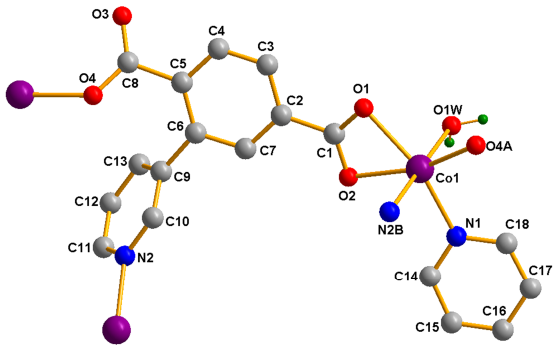

Fig. S3 The ball-and-stick drawing of the asymmetric unit in **2**, the hydrogen atoms and solvent molecules are omitted. Symmetry codes: A: -1/2+x, 1/2-y, -1/2+z; B: -x, y, 1/2-z.

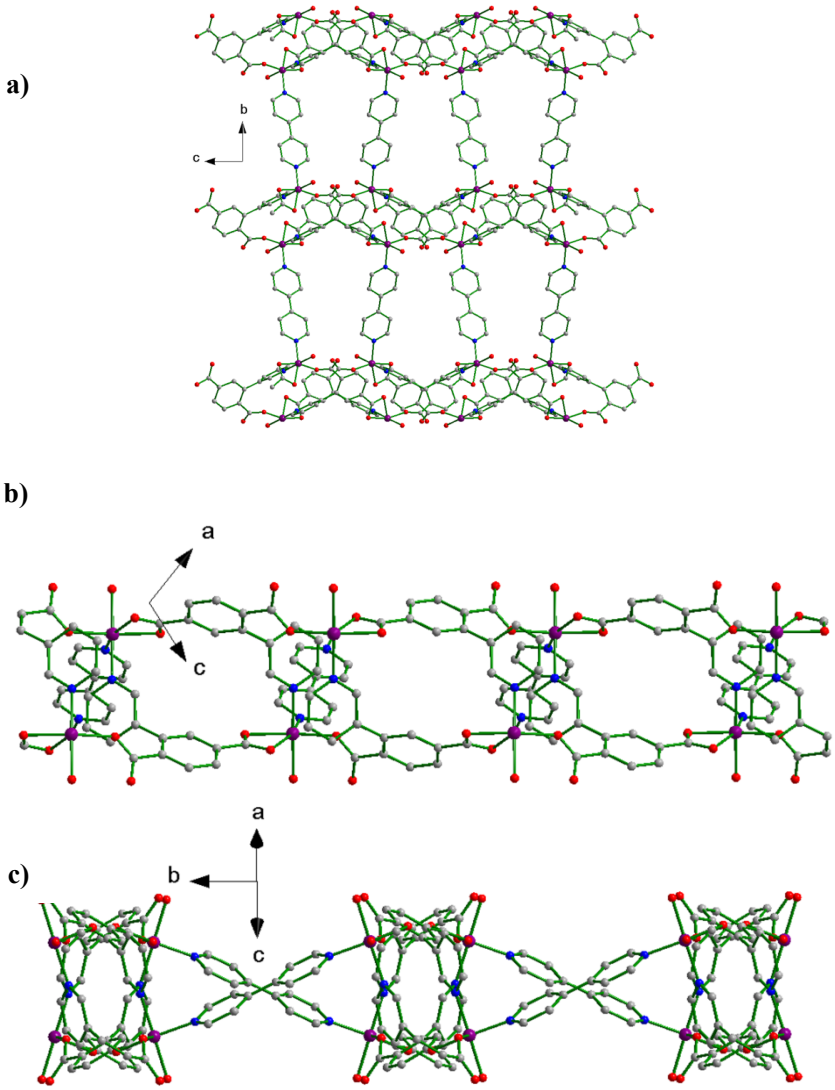

Fig. S4 View of the 2D layer of **2**: a) along the crystallographic *a*-axis; b) along the crystallographic *b*-axis; c) along the crystallographic (101)-axis.

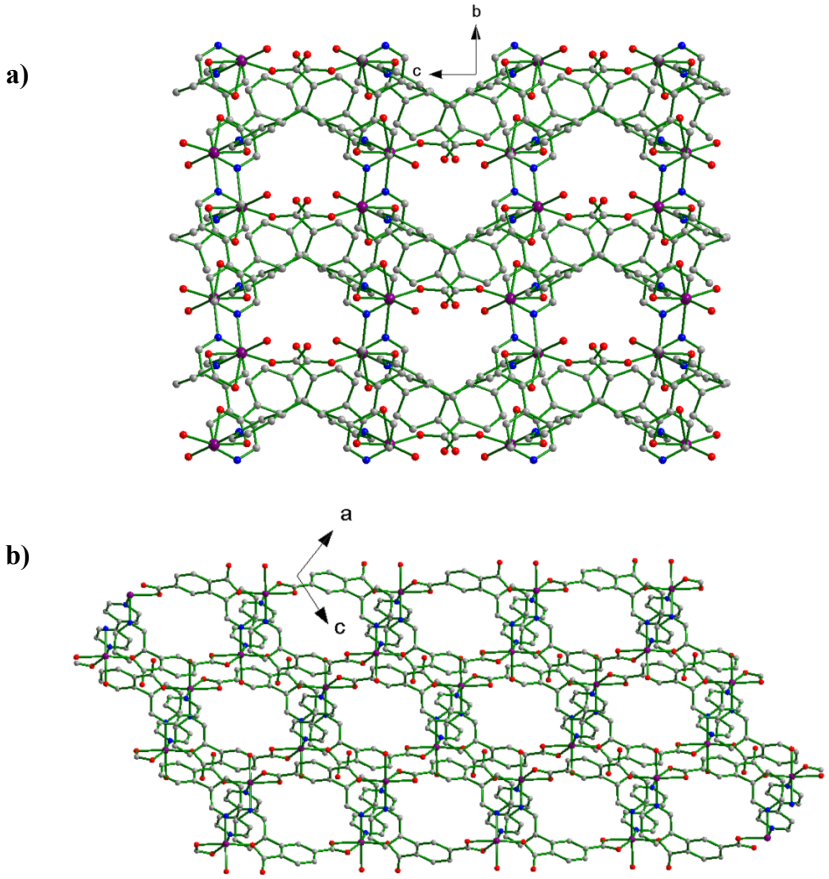

Fig. S5 View of the 2D stacked layers of **2**: a) along the crystallographic (100)-axis; b) along the crystallographic (010)-axis.

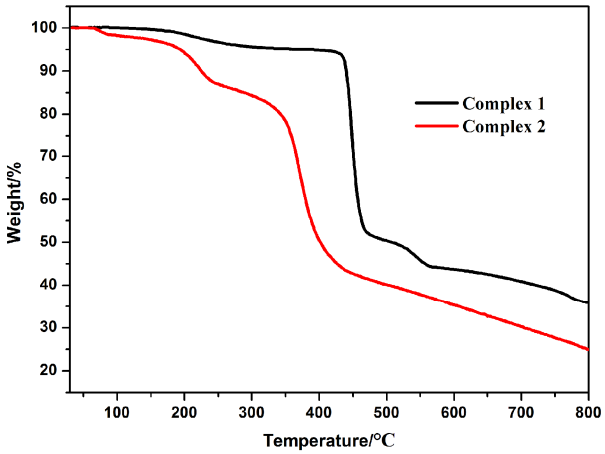

Fig. S6. TGA curves for **1** and **2** measured under nitrogen.

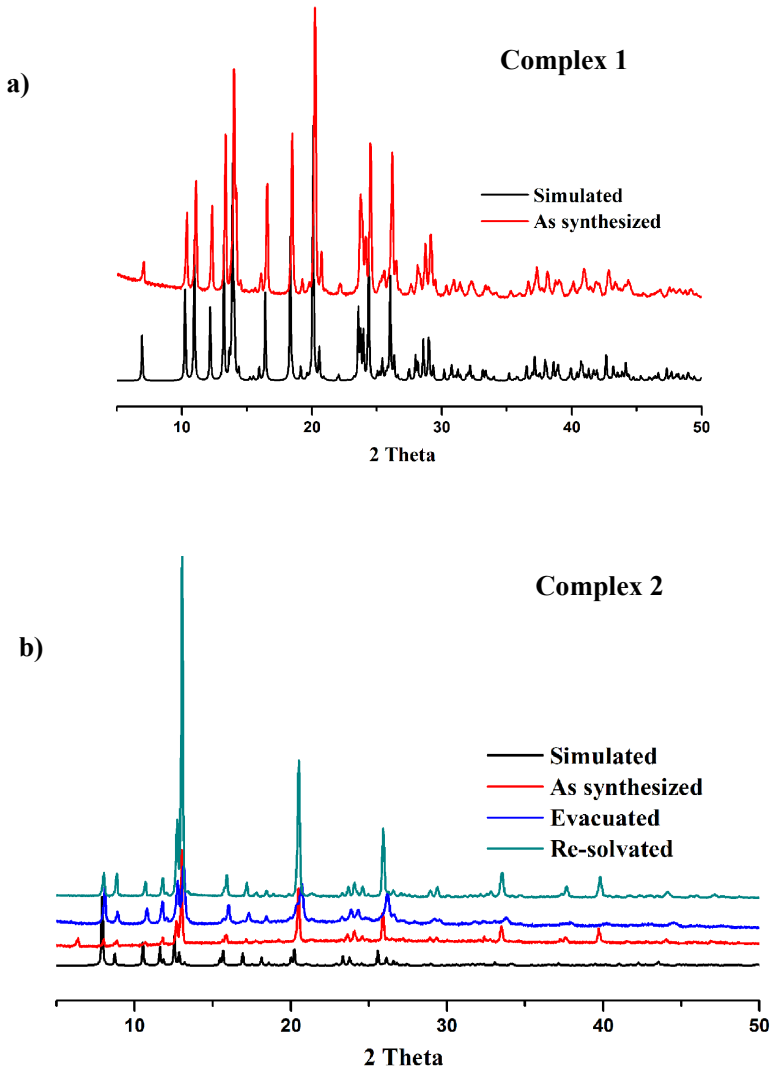

Fig. S7 PXRD patterns of **1** simulated from the X-ray single-crystal structure and as-synthesized a), and **2** simulated from the X-ray single-crystal structure, as-synthesized, desolvated and resolvated samples b).

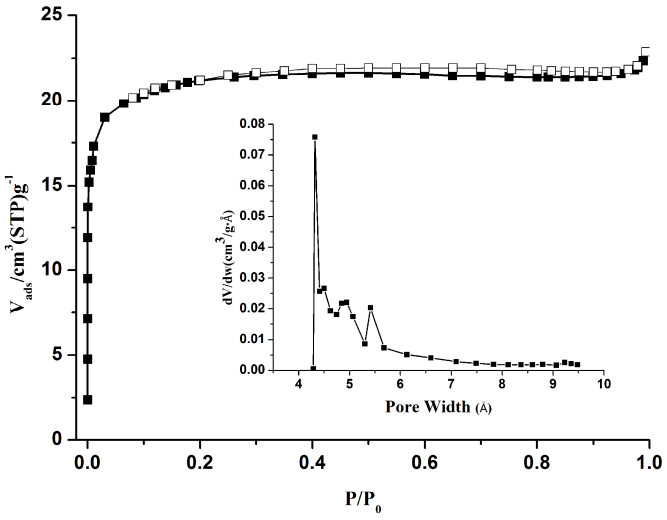

Fig. S8 Differential pore volume as a function of pore width calculated from the adsorption isotherm of Ar at 87 K using the Horvath-Kawazoe model, median pore width of 4.95 Å.

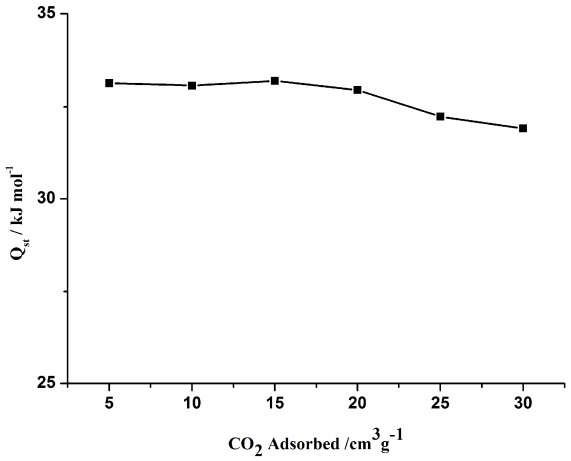

Fig. S9 Isosteric heat of adsorption for CO_2 at different CO_2 loadings in **2**.

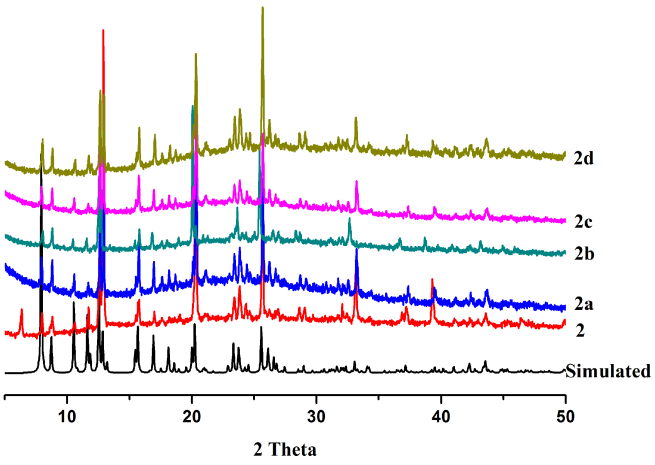

Fig. S10 PXRD patterns for complexes **2, 2a, 2b, 2c and 2d**.

Table S1. Crystal data and structure refinements for **1**, **2**, **2a**, **2b**, **2c** and **2d**.

Complex No.	**1**	**2**	**2a**	**2b**
Empirical formula	$C_{18}H_{13}N_2CoO_5$	$C_{18}H_{17}N_2CoO_7$	$C_{18}H_{17}N_2CoO_7$	$C_{18}H_{17}N_2CoO_7$
Formula mass	396.22	432.23	432.23	432.23
Temperature [K]	296(2)	296(2)	296(2)	296(2)
Crystal system	monoclinic	monoclinic	monoclinic	monoclinic
Space group	*P2/c*	*C2/c*	*C2/c*	*C2/c*
a [Å]	13.1622(15)	17.795(2)	17.777(3)	17.877(4)
b [Å]	7.2427(8)	14.8776(19)	14.926(3)	14.730(3)
c [Å]	17.7408(19)	16.052(2)	16.131(3)	16.583(3)
β [º]	103.584(2)	109.140(2)	109.324(3)	109.764(4)
V [Å^3]	1643.9(3)	4014.8(8)	4039.1(13)	4109.5(14)
Z	4	8	8	8
$D_{calcd.}$[g·cm^{-3}]	1.593	1.417	1.408	1.384
μ [mm^{-1}]	1.077	0.895	0.890	0.874
GOF on F^2	1.044	1.088	1.053	1.054
reflns collected/ unique	8007/2928	10042/3578	11741/4603	10135/3660
R_{int}	0.0297	0.0499	0.0907	0.0756
Final R[a] indices [I>2σ(I)]	R_1 = 0.0353 wR_2 = 0.0901	R_1 = 0.0611 wR_2 = 0.1845	R_1 = 0.0775 wR_2 = 0.1996	R_1 = 0.0793 wR_2 = 0.2039

Complex No.	**2c**	**2d**
Empirical formula	$C_{36}H_{32}Co_2N_4O_{13}$	$C_{36}H_{32}Co_2N_4O_{13}$
Formula mass	846.47	846.47
Temperature [K]	296(2)	296(2)
Crystal system	monoclinic	monoclinic
Space group	*C2/c*	*C2/c*
a [Å]	17.7715(12)	17.547(10)
b [Å]	14.9149(10)	14.908(9)
c [Å]	16.1199(11)	16.176(10)
β [º]	109.3020	108.365(9)
V [Å^3]	4032.6(5)	4016(4)
Z	4	4
$D_{calcd.}$[g·cm^{-3}]	1.384	1.390
μ [mm^{-1}]	0.888	0.892
GOF on F^2	1.001	1.006
reflns collected/ unique	11146/3526	8601/3560
R_{int}	0.0296	0.0751
Final R[a] indices [I>2σ(I)]	R_1 = 0.0656 wR_2 = 0.1906	R_1 = 0.0826 wR_2 = 0.2110

[a] $R_1=\sum||F_o|-|F_c||/\sum|F_o|$, $wR_2=[\sum w(F_o^2- F_c^2)^2/ \sum w(F_o^2)^2]^{1/2}$